

MULTI-LAYER SUBSTRATE INTEGRATED WAVEGUIDE *E*-PLANE POWER DIVIDER

P. Mohammadi^{1, 2} and S. Demir^{2, *}

¹Department of Electrical and Electronic Engineering, Islamic Azad University, Urmia Branch, Urmia, Iran

²Department of Electrical and Electronic Engineering, Middle East Technical University, Ankara, Turkey

Abstract—A new multilayer power divider with Substrate Integrated Waveguide (SIW) technology is proposed. In this work, two-way and four-way power divider realizations by two-layer and three-layer SIW, respectively, are presented. Considering the small size of the structure, extension of this method to n -way power dividers and antenna feed networks are possible, and it has the potential for integration of compact multi-layer SIW circuits. Due to the lack of a multiport counterpart of the two-port thru-reflect-line (TRL) calibration, scattering matrix of an n -way power divider must be reconstructed from measured data. A method is introduced for reconstruction of S -parameters of the n -port non-coaxial device with a two-port vector network analyzer (VNA). The two-way power divider is designed for 9–10.5 GHz band. Transmission coefficient about -3.5 dB and return loss below -10 dB has been measured for this two-way power divider. For four-way power divider, transmission about -7 dB in the 9.5–10.5 GHz has been achieved.

1. INTRODUCTION

Power dividers are building blocks of many microwave and millimeter wave integrated circuits and systems. Antenna feed networks are one of these applications. In general, Substrate Integrated Waveguide (SIW) has a relatively large footprint compared to conventional printed circuit counterparts. Some advantages such as being low cost, low loss and suitable for high density integration with microwave and millimeter wave component popularized SIW in the past few

Received 29 April 2012, Accepted 4 June 2012, Scheduled 16 June 2012

* Corresponding author: Simsek Demir (simsek@metu.edu.tr).

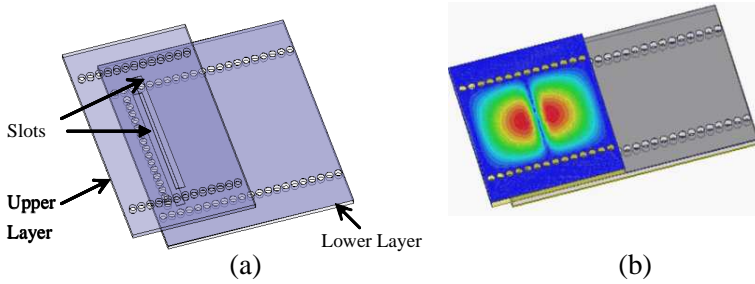


Figure 1. The main structure of multi-layer SIW. (a) First and second layers with slots. (b) The coupled E -fields.

years [1–7]. Conventional technologies for designing high quality power dividers, including a metal rectangular waveguide or microstrip line are either bulky or unable to provide low insertion loss. An acceptable performance with considerably decreased size can be offered by SIW technology as a potential solution to the compact communication applications. Moreover, multilayer SIW keeps all the advantages of conventional multilayer PCB structure and will further resolve the problem of radiation from the microstrip feed lines due to its closed structure. Several power dividers based on SIW have been reported [3–5]. However, these SIW power dividers in the multi-way port environment suffer from large size due to lateral port distribution. The low profile property of SIW is utilized in [4] by developing a multilayer structure, somewhat similar to the presented configuration in the current study. However, this study is much more convenient for applications like antenna array feed network designs.

The main structure of new multilayer SIW power divider is shown in Fig. 1 [7]. There are two layers which are attached together. The electromagnetic wave is coupled from the first layer to the second layer through a slot. This idea is used for increasing the output ports by increasing the number of layers and slots in each coupling layer without increasing the width of structure.

The electrical behavior of SIW is similar to rectangular waveguide. By using the well-known rectangular waveguide equations and introducing SIW parameters (e.g., via diameter and distance between vias), the equivalent width of SIW can be calculated for the desired response in the frequency band of interest.

The SIW component must be interconnected with a planar structure in order to provide means for measurement with a vector network analyzer (VNA). The tapered microstrip transition has widely

been adopted [8]. Design equations for tapered microstrip transition are given in [9]. However, measuring the whole SIW structure without tapered microstrip transition is a matter of concern here. This leads us to use of thru-reflect-line (TRL) [10] calibration technique for measuring the S -parameters of the whole SIW structure. With the use of TRL calibration function and appropriate TRL standards, a modern VNA can measure a two-port DUT in a desired reference plan. Nevertheless, due to the lack of an established multiport counterpart of the two-port TRL, a method for measuring the multiport non-coaxial DUT up to the intrinsic ports is developed. This method has been applied for reconstruction of S -parameters of the two-way and four-way SIW power dividers. Comparison of this method with available methods shows that its complexity is less than similar methods. Also the desired S -parameters can be constructed individually, while other methods reconstruct all the parameters simultaneously and need more complex matrix calculations.

2. DESIGN OF THE SIW POWER DIVIDER

2.1. SIW Design

SIW is a quasi-rectangular waveguide formed by periodic via-hole connection between two metal layers and TE_{10} is the dominant mode. With the knowledge of the pitch between consecutive vias and via diameters, SIW can be replaced by an equivalent dielectric filled rectangular waveguide. The equivalent width (a_e) is computed using the method presented in [11]. The cut-off frequency for rectangular waveguide is given as follows:

$$f_{cmn} = \frac{k_c}{2\pi\sqrt{\mu\epsilon}} = \frac{1}{2\pi\sqrt{\mu\epsilon}} \sqrt{\left(\frac{m\pi}{a_e}\right)^2 + \left(\frac{n\pi}{b}\right)^2} \quad (1)$$

$$f_{c10} = \frac{1}{2a_e\sqrt{\mu\epsilon}} \quad (2)$$

where b is the substrate thickness, a_e is the equivalent width of SIW, μ and ϵ are the permittivity and permeability of the substrate, respectively.

2.2. Power Divider Design

The similarity of SIW power divider in Fig. 1 with E -plane power divider encourages the use of E -plane power divider design procedure for designing SIW counterpart. E -plane power divider and its equivalent SIW power divider is shown in Fig. 2 [12].

The reactive effect associated with the localized higher-mode can be accounted in the equivalent circuit. The data in [12] indicate that for $b \leq b'$, X is quite small and negligible. For SIW structure b' is the substrate thickness, and $b = b'$.

$$Z_o = \frac{b}{a} \frac{\sqrt{\mu_r} \lambda_g}{\sqrt{\epsilon_r} \lambda} \quad (3)$$

is the characteristic impedance of the rectangular waveguide and n can be calculated from [12]. For SIW power divider in Fig. 1 Z'_o is the characteristic impedance of the input line (first layer) and Z_o is the characteristic impedance of the two output lines (second layer). For the SIW equivalent circuit in Fig. 2(c) $b = b'$ is the substrate thickness, so the width of the SIW, a , is the only variable to achieve the desired response. The design steps for SIW power divider are as follows:

1- The first layer width is determined by cut-off frequency in (2) and the characteristic impedance of first layer, Z'_o , is calculated from (3).

2- The characteristic impedance of the second layer Z_o is calculated from equivalent circuit for matching the input ports.

3- Width of the second layer is calculated from (3).

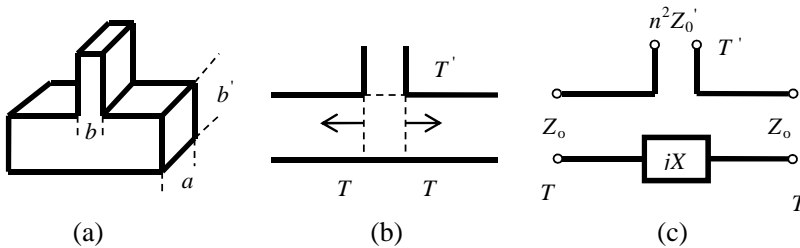


Figure 2. *E*-plane power divider. (a) General view. (b) Side view. (c) Equivalent circuit.

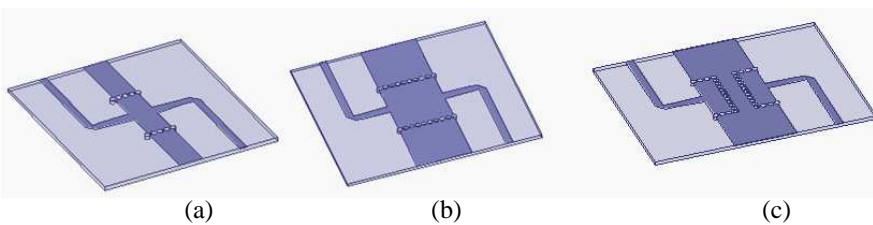


Figure 3. Standards for SIW power divider. (a) Thru. (b) Line. (c) Reflect.

It is possible to use this design procedure for the n -way power divider by increasing the number of layers.

2.3. TRL Calibration

The S -parameters of SIW power divider without the microstrip transition parts are achievable in the light of TRL calibration technique. The three TRL standards for SIW structure are shown in Fig. 3. For avoiding any radiation effects the reflect standard is a short circuit. The through standard is made by connecting two error boxes directly together. The design steps for SIW power divider is continued as follows:

- 4- TRL standards are designed.
- 5- Transition part is calculated from [8] by considering the width of the input port.

2.4. TRL Measurement of Non-coaxial Multiport Device with Two-port VNA

A modern VNA with TRL calibration and appropriate standards can measure two-port non-coaxial DUT at desired reference planes. In contrast, due to lack of a multiport counterpart of a full two-port TRL calibration, a multiport VNA cannot measure a multiport non-coaxial DUT up to the intrinsic ports as straightforwardly as measuring the coaxial one. In [13,14] the n -port scattering matrix is calculated directly from C_2^m set of two-port scattering matrix. In [15] the n -port scattering matrix can be reconstructed from n sets of reduced $(n - 1)$ -ports scattering matrix by connecting the known termination to each port one at a time. This reduction process can be continued to reduce the port order, and the resulting minimal reduced port order is three. Both of these methods need more complex matrix calculation. In the

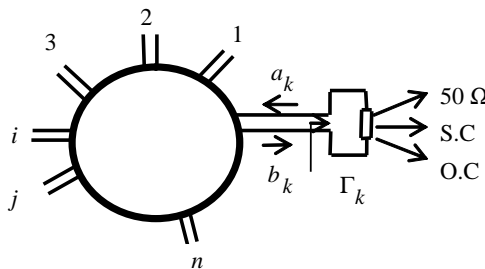


Figure 4. An n -port network with three different loads connection.

following a new method will be introduced which has less mathematical calculation and each scattering matrix will be calculated individually.

An n -port network with a termination (with a reflection coefficient Γ_k) that is connected at the k th port is shown in Fig. 4. All other ports are connected to $50\ \Omega$. The relationship between $S_{ij}^{(k)}$ (measurement scattering matrix) of this reduced $(n-1)$ port network and S_{ij} (true scattering matrix) of this n -port network is given as [15]:

$$S_{ij}^{(k)} = S_{ij} + \frac{S_{ik}S_{kj}\Gamma_k}{1 - S_{kk}\Gamma_k} \quad i, j, k = 1, \dots, n \quad i, j \neq k \quad (4)$$

This formula can be applied for the three different loads, the results are given below:

a) $50\ \Omega$ termination

$$S_{ij\alpha}^{(k)} = S_{ij} + \frac{S_{ik}S_{kj}\Gamma_\alpha}{1 - S_{kk}\Gamma_\alpha} \quad k \neq i, j \quad (5)$$

b) Short circuit (S. C.) termination

$$S_{ij\beta}^{(k)} = S_{ij} + \frac{S_{ik}S_{kj}\Gamma_\beta}{1 - S_{kk}\Gamma_\beta} \quad k \neq i, j \quad (6)$$

c) Open circuit (O. C.) Termination

$$S_{ij\theta}^{(k)} = S_{ij} + \frac{S_{ik}S_{kj}\Gamma_\theta}{1 - S_{kk}\Gamma_\theta} \quad k \neq i, j \quad (7)$$

From (5)–(7), the two unknown, S_{ij} and S_{kk} , can be derived as follows.

$$S_{kk} = \frac{A(\Gamma_\alpha - \Gamma_\theta) - (\Gamma_\alpha - \Gamma_\beta)}{A\Gamma_\beta(\Gamma_\alpha - \Gamma_\theta) - \Gamma_\theta(\Gamma_\alpha - \Gamma_\beta)} \quad A = \frac{S_{ij\alpha}^{(k)} - S_{ij\beta}^{(k)}}{S_{ij\alpha}^{(k)} - S_{ij\theta}^{(k)}} \quad k \neq i, j \quad (8)$$

$$S_{ik}S_{kj} = \frac{(S_{ij\alpha}^{(k)} - S_{ij\beta}^{(k)}) (1 - S_{kk}\Gamma_\alpha) (1 - S_{kk}\Gamma_\alpha)}{\Gamma_\alpha - \Gamma_\beta} \quad (9)$$

$$S_{ij} = S_{ij\alpha}^{(k)} - \frac{S_{ik}S_{kj}\Gamma_\alpha}{1 - S_{kk}\Gamma_\alpha} \quad k \neq i, j \quad (10)$$

Γ_α , Γ_β , Γ_θ are reflection coefficients of port k when it is connected to $50\ \Omega$, S. C. and O. C. loads, respectively. For SIW structure reflection coefficients for different loads can be found from TRL standard [16]. Thus, when the return loss from port k is needed, it is sufficient to connect 3 different loads to it and do measurement from any two other ports. Comparison of this method with the method in [17] shows that we can find the desired S -parameter individually, but in other method all parameters will be found simultaneously. And the situation becomes worse when the number of ports increases.

3. EXPERIMENTAL RESULTS

3.1. Two-way SIW Power Divider

Two-way SIW power divider is shown in Fig. 5. By applying the design procedure steps for the two-way power divider in Fig. 5, dimensions

Table 1. Two-way SIW power divider dimensions(mm).

	Length	Width
First Layer (L_1)	4	9.1
Second Layer (L_2)	9	11.5
Slot	8	1
Transition Part	4.6	1.5

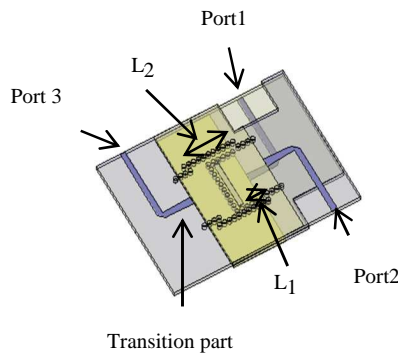


Figure 5. Two-way SIW power divider.

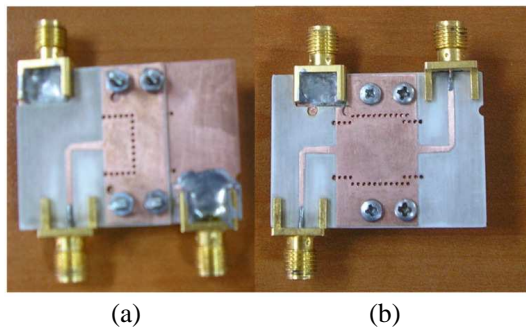


Figure 6. Two-way SIW power divider. (a) Bottom view. (b) Top view.

can be found as shown in Table 1. As seen in the figure, output widths of all the ports are the same. This intentional choice eases the TRL calibration for the S -parameters of the whole SIW power divider. Via diameter is 0.8 mm and separation between vias is 0.2 mm. Picture of the fabricated SIW is given in Fig. 6.

The measurement process for the two-way SIW is visualized in Fig. 7. As stated in Section 2.4, measurement of $S_{ij}^{(k)}$ and Γ_k are required for the reconstruction calculations. TRL measurement setup for calculating the return loss (S_{11}) and the transmission coefficients (S_{21} and S_{31}) is shown in Fig. 7(a). By connecting three different loads to Thru (Fig. 7(b)) three reflection coefficients ($\Gamma_\infty, \Gamma_\beta, \Gamma_\theta$) are measured.

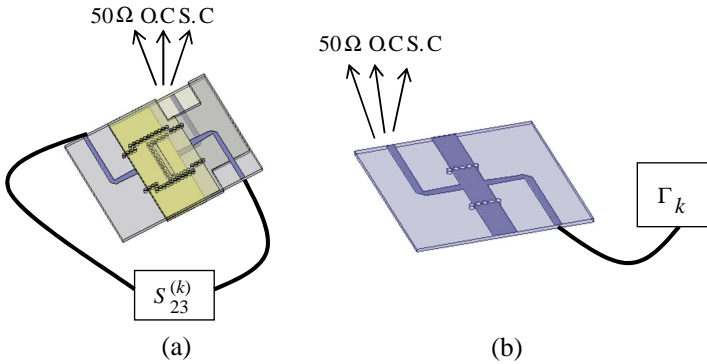


Figure 7. (a) Measurement setup for return loss and transmission coefficient reconstruction. (b) Reflection coefficient measurement from through standard.

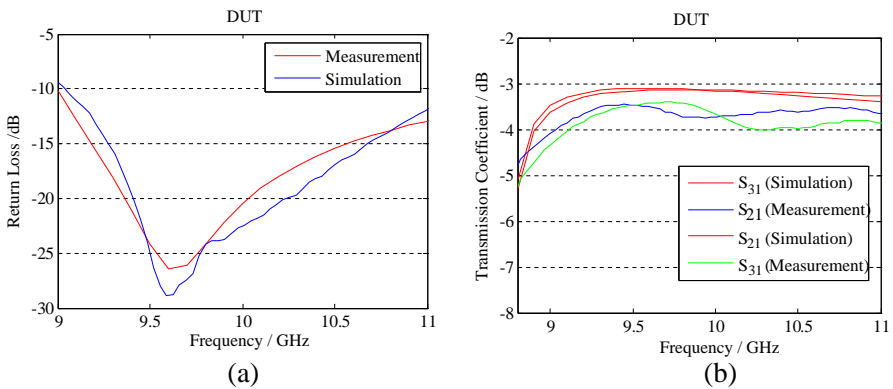


Figure 8. Simulation and measurement result for two-way SIW power divider. (a) Return loss. (b) Transmission coefficients.

Simulation and reconstructed results are shown in Fig. 8. Constructed measurement results of DUT have been achieved based on TRL calibration, and by applying the method explained in Section 2.4.

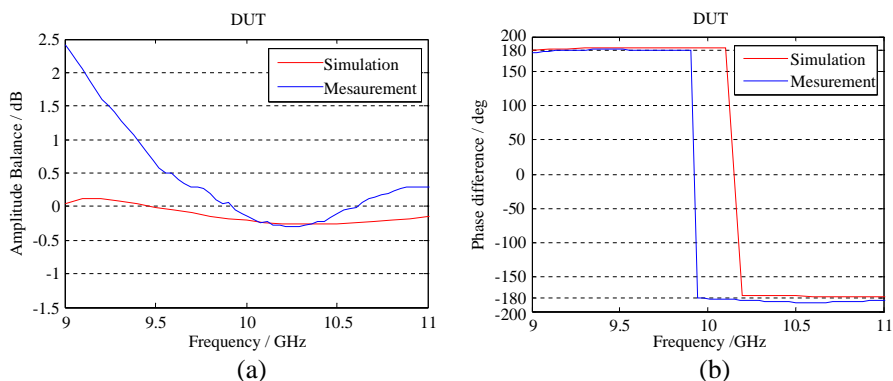


Figure 9. (a) Amplitude balance. (b) Phase difference of 3-port SIW power divider.

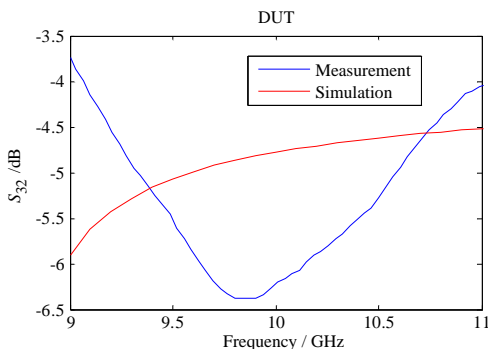


Figure 10. Isolation of 3port SIW power divider.

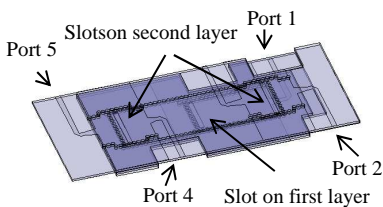


Figure 11. Four-way SIW power divider.

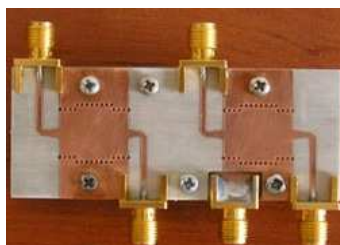


Figure 12. Picture of the four-way SIW power divider.

These results show that return loss is below -10 dB between 9–11 GHz and also transmission coefficient is about -3.5 dB and -4 dB for the same frequency band. As shown in Fig. 9 the measured amplitude imbalance is about ± 0.5 dB from 9.5 GHz to 11 GHz. The measured phase difference between $\angle S_{21}$ and $\angle S_{31}$ is about $\pm 4^\circ$ in the same frequency bandwidth. This shows that the amplitude and phase balance is acceptable. Fig. 10 shows the isolation between output ports; isolation is consistent with the expectations. Since there is no isolation resistance between the output ports, isolation is not high. However, as for a beam forming network, this is not critical in certain applications.

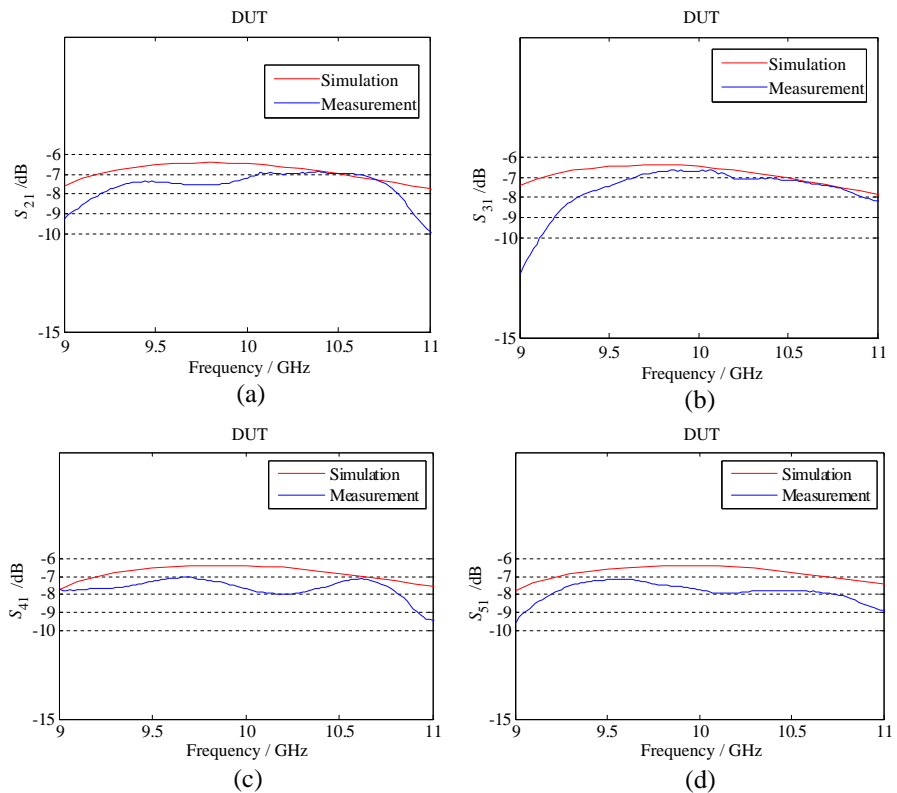


Figure 13. The simulation and measurement results of four-port SIW power divider. (a) S_{21} . (b) S_{31} . (c) S_{41} . (d) S_{51} .

3.2. Four-way SIW Power Divider

A four-way SIW power divider is designed using the procedure in Section 2. As shown in Fig. 11 it includes three layers. For coupling the electromagnetic wave between layers, three slots are used, one of them is in the first layer and two others are in the second layer. Similar to two-way SIW power divider, after TRL calibration, measurement reconstruction procedure based on (4) and (5) is utilized. The picture of the fabricated design is shown in Fig. 12.

Four-way SIW power divider dimensions are given in Table 2. The diameter of a via and the distance between two adjacent vias, and also the slots dimensions are the same as the two-way SIW power divider. The simulation and measurement results of the four-way SIW power divider are shown in Fig. 13. A good agreement is seen between simulation and measurement results of DUT in 9.5–10.5 GHz where measurement data are obtained based on TRL calibration and reconstruction. The measured amplitude difference and phase difference between S_{21} and S_{31} of the 5-port SIW power divider are

Table 2. Four-way SIW power divider dimension (mm).

	Length	Width
First Layer	8.2	9
Second Layer	32	11
Third Layer	7	11
Transition Part	2.64	2

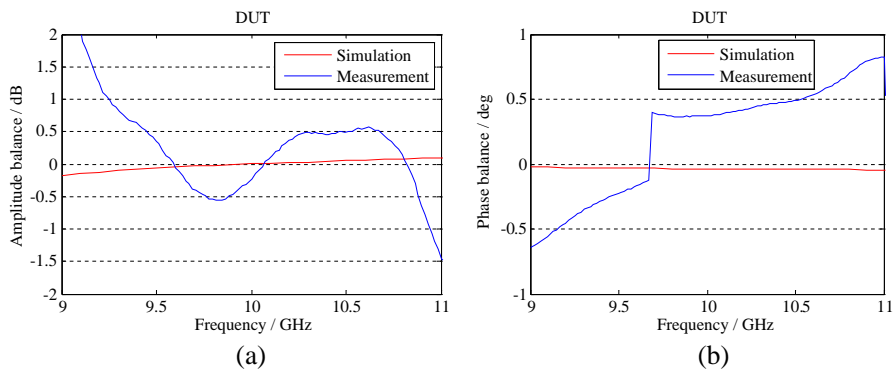


Figure 14. (a) Amplitude balance. (b) Phase difference of 5-port SIW power divider.

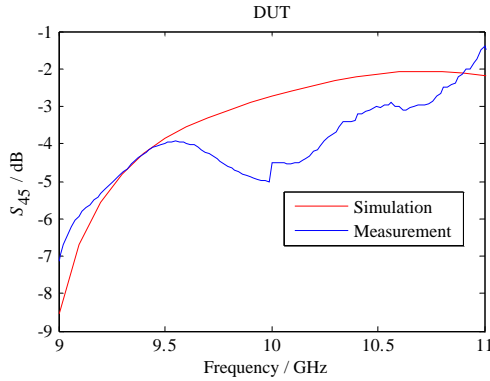


Figure 15. Isolation of 5-port SIW power divider.

shown in Figs. 14(a) and (b), respectively. Amplitude imbalance is about ± 0.5 dB from 9.5 GHz to 11 GHz, and phase imbalance is approximately $\pm 0.5^\circ$. Isolation in Fig. 15 is as expected due to absence of resistance between output ports.

4. CONCLUSION

In this paper a novel SIW n -way power divider design method is proposed. This method is applied for two-way and four-way dividers. The simulation and measurement results of DUT show good agreement. The same method can be developed for 2^n -way arrangement. The small size of the structure is attractive for compact feed network applications.

A new method for reconstruction of S -parameters from measured data is also presented for n -way networks. Comparison of this reconstruction method with available methods shows that it can be applied for rebuilding the desired S -parameters individually without complicated calculations.

REFERENCES

1. Wu, K., D. Deslandes, and Y. Cassivi, "The substrate integrated circuits — A new concept for high-frequency electronics and optoelectronics," *6th International Conference on Telecommunications in Modern Satellite, Cable and Broadcasting Service, TELSIKS 2003*, Vol. 1, P-III-P-X, Oct. 1–3, 2003.
2. Zhang, Q.-L., W.-Y. Yin, S. He, and L.-S. Wu, "Evanescent-mode substrate integrated waveguide (SIW) filters implemented with

- complementary split ring resonators,” *Progress In Electromagnetics Research*, Vol. 111, 419–432, 2011.
3. Song, K., Y. Fan, and Y. Zhang, “Eight-way substrate integrated waveguide power divider with low insertion loss,” *IEEE Transactions on Microwave Theory and Techniques*, Vol. 56, No. 6, 1473–1477, Jun. 2008.
 4. Eom, D., J. Byun, and H. Y. Lee, “Multi-layer four-way out-of-phase power divider for substrate integrated waveguide applications,” *2009 IEEE MTT-S International Microwave Symposium Digest (MTT)*, 477–480, Jun. 7–12, 2009.
 5. Seo, T. Y., J. W. Lee, C. Cho, and T. K. Lee, “Radial guided 4-way unequal power divider using substrate integrated waveguide with center-fed structure,” *Asia Pacific Microwave Conference, APMC 2009*, 2758–2761, Dec. 7–10, 2009.
 6. Bakhtafrooz, A., A. Borji, D. Busuioc, and S. Safavi-Naeini, “Novel two-layer millimeter-wave slot array antennas based on substrate integrated waveguides,” *Progress In Electromagnetics Research*, Vol. 109, 475–491, 2010.
 7. Mohammadi, P. and S. Demir, “Two layers substrate integrated waveguide power divider,” *General Assembly and Scientific Symposium, 2011 XXXth URSI*, 1–4, Aug. 13–20, 2011.
 8. Deslandes, D. and K. Wu, “Integrated microstrip and rectangular waveguide in planar form,” *IEEE Microwave and Wireless Components Letters*, Vol. 11, No. 2, 68–70, Feb. 2001.
 9. Deslandes, D., “Design equations for tapered microstrip-to-substrate integrated waveguide transitions,” *2010 IEEE MTT-S International Microwave Symposium Digest (MTT)*, 704–707, May 23–28, 2010.
 10. Pozar, D. M., *Microwave Engineering*, 3rd Edition, John Wiley & Sons, 2005.
 11. Xu, X., R. G. Bosisio, and K. Wu, “A new six-port junction based on substrate integrated waveguide technology,” *IEEE Transactions on Microwave Theory and Techniques*, Vol. 53, No. 7, 2267–2273, Jul. 2005.
 12. Marcuvitz, N., *Waveguide Handbook*, 336–350, McGraw-Hill Book Company, Inc., 1951.
 13. Tippet, J. C. and R. A. Speciale, “A rigorous technique for measuring the scattering matrix of a multiport device with a 2-port network analyzer,” *IEEE Transactions on Microwave Theory and Techniques*, Vol. 30, No. 5, 661–666, May 1982.
 14. Lin, W. and C. Ruan, “Measurement and calibration of a universal

- six-port network analyzer,” *IEEE Transactions on Microwave Theory and Techniques*, Vol. 37, No. 4, 734–742, Apr. 1989.
15. Lu, H.-C. and T.-H. Chu, “Multiport scattering matrix measurement using a reduced-port network analyzer,” *IEEE Transactions on Microwave Theory and Techniques*, Vol. 51, No. 5, 1525–1533, May 2003.
 16. Chen, C.-J. and T.-H. Chu, “Measurement of noncoaxial multiport devices up to the intrinsic ports,” *IEEE Transactions on Microwave Theory and Techniques*, Vol. 57, No. 5, 1230–1236, May 2009.
 17. Sercu, S. and L. Martens, “Characterizing n -port packages and interconnections with a 2-port network analyzer,” *IEEE 6th Topical Meeting on Electrical Performance of Electronic Packaging*, 163–166, Oct. 27–29, 1997.